Int. J. Electrochem. Sci., 15 **(2020)** 4556 – 4566, doi: 10.20964/2020.05.09

International Journal of
ELECTROCHEMICAL
SCIENCE
www.electrochemsci.org

Preparation of DNA-Based Biosensor for Electrochemically Identification of Transgenic Soybean

Yuanxi Deng[1*], *Jie Wu*[1], *Kang Tu*[2*], *Hui Xu*[1], *Long Ma*[1], *Jia Chen*[1] and *Jialiang Wang*[1]

[1] College of Food and Bioengineering, Bengbu University, Anhui, 233030. P.R. China
[2] College of Food Science and Technology, Nanjing Agricultural University, Jiangsu, 210095, P.R. China
[*]E-mail: Yuanxi Deng: 278967574@qq.com Kang Tu: Kangtu163@foxmail.com

Received: 24 December 2019 / *Accepted:* 3 February 2020 / *Published:* 10 April 2020

Since the successful transformation of the first transgenic soybean, the variety and planting area of transgenic soybean have increased. Therefore, transgenic soybean identification has become a necessary procedure in gm research. The development of rapid, sensitive, high-throughput and newly automated detection methods has become a hot spot in the detection of transgenic products. In this paper, we modified a layer of a partially reduced graphene oxide film on the surface of an ionic liquid carbon paste electrode by a green, controlled electrochemical reduction method. We fixed the probe on the electrode surface by covalently bonding the remaining oxygen-containing groups on the electrode surface with an end-modified amino group. Then, the hybridization reaction was detected with methylene blue as an indicator after hybridization between the electrode and the target sequence, and the transgenic soybean sequence was detected by differential pulse voltammetry. We also tested PCR products of DNA extracted from actual samples.

Keywords: Graphene oxide; Electroreduction; DNA sensor; Transgenic soybean; Surface modification

1. INTRODUCTION

DNA is the carrier of genetic information and has the function of transmitting and storing information. DNA exists in any organism, virus or pathogen, which is of great significance for the detection and diagnosis of various diseases. Because DNA plays an important role in medical diagnosis, environmental monitoring, forensic identification and food hygiene inspection, how to detect specific DNA sequences quickly and accurately is of great significance. Electrochemical DNA sensors have a series of advantages, such as being fast, simple, and sensitive, while also having high selectivity, operational simplicity and a low cost [1–4]. It has wide application prospects in many fields. An

electrochemical DNA sensor uses the electrode as a transducer. Under certain conditions, a single strand DNA probe is fixed on the surface of the working electrode by certain methods [5–8]. Under appropriate conditions, it hybridizes with a complementary sequence in a solution to form double-stranded DNA by the complementary pairing of bases between the DNA chains. Then, an electrochemical method is used to detect the changes in electrochemical signals before and after hybridization [9–11]. By using the qualitative detection of a specific target gene sequence and the linear relationship between the electrochemical signal and the concentration of the target, we can achieve the quantitative detection of a specific DNA sequence [12–16].

The main steps for preparing the electrochemical DNA sensor are as follows: ① fix the probe ssDNA on the electrode surface; ② hybridize with the target ssDNA sequence; ③ indicate the hybridization reaction; and ④ analyze the electrochemical detection of the hybridization signal. The most important part is the fixation of probe ssDNA and the hybridization detection. The amount of probe ssDNA fixed on the electrode surface and the detection method of the hybridization reaction will affect the sensitivity of the sensor [17–20]. To ensure the sensitivity and reproducibility of the sensor, a probe array plays an important role in the preparation of the sensor. Commonly used working electrodes in electrochemical sensors are glassy carbon electrodes, gold electrodes, carbon paste electrodes and pyrolytic graphite electrodes. Generally, the methods to determine the probe on the surface of solid electrodes include adsorption, covalent bonding, self-assembly and biotin avidin [21–24]. Electrochemical methods can be used to detect DNA pairs from two aspects: one is that the base contained in the molecule itself has electrochemical activity, which is the basis of early research on the Lai electrode; and the other is that the complementary pairing between two single strands of DNA can cause a change in the DNA itself or the corresponding electrochemical indicator signal that detects the DNA [25–31].

Electrochemical sensors have been widely used in environmental detection, food detection, drug detection, clinical disease diagnosis and new drug development [32,33]. In addition to these applications, electrochemical DNA sensors have also been used for the identification of transgenic products [32,34–40]. Despite the rapid development of transgenic technology in recent years, the growing area of transgenic crops is expanding, but the safety of transgenic crops has always been the focus of controversy. There are many detection methods for transgenes [41–43], but the most common methods are PCR and FQ-PCR. In addition, in recent years, the emergence of new methods of transgenic detection has enriched and improved the detection system of genetically modified food [44–46]. In the 1980s, Monsanto Company obtained EPSP resistance genes from Petunia. By using Ti plasmid-mediated transfer DNA technology, the EPSP gene controlled by p35s in the Petunia plasmid was introduced into the soybean genome, and then a transgenic soybean variety resistant to a glyphosate herbicide was developed. Genetically modified soybean was approved in the United States in 1994 and became one of the first genetically modified crops to be commercialized. Genetically modified soybean has the following incomparable advantages: reduces the use of pesticides, avoids environmental pollution, increases production, solves the problem of food shortage, reduces production costs, reduces food prices, increases food nutrition, improves added value, promotes production efficiency and promotes agricultural development [47–49]. Although transgenic soybean have been widely introduced into the market, people still have doubts about the safety and reliability of transgenic soybean, so the detection

of transgenic soybean is essential [50–52]. The existing detection methods cannot meet the increasing needs of detection. It is urgent to develop rapid detection methods with high sensitivity, high specificity, high efficiency and high throughput.

Under certain conditions, graphite can react with strong oxidants. After being oxidized, there are hydroxyl, epoxy, carboxyl and carbonyl groups on its surface and edge. At the same time, the gap between the graphite layers increases, and the product becomes graphite oxide. Thin graphite oxide (GO) can be obtained by applying a certain external force to destroy the van der Waals force between the layers. The methods of obtaining GO from graphite oxide are pyrolytic expansion, ultrasonic dispersion, electrostatic repulsion and low-temperature stripping. Among them, ultrasonic dispersion is the most commonly used method, and GO produced after ultrasonic stripping can be dispersed in common solvents to form a stable GO solution. Graphite has excellent physical and chemical properties and wide application prospects. Thin graphite layers are connected together by strong van der Waals forces. Without the existence of external protectors, thin graphite layers easily agglomerate, making it difficult to disperse in common solvents, thus affecting the application prospect of graphite refining. Therefore, it is necessary to functionalize graphite to improve its dispersion and stability in a solvent and to effectively control its performance and structure to achieve more functions and applications. Second, the introduction of specific chemical groups or functional molecules through functionalization can also give more properties to the refined graphite or graphite oxide. There are two kinds of functionalization of graphite: one is functionalization on the basis of thin graphite, the other is functionalization of thin graphite oxide, which is then reduced. Functional graphite oxide can also be obtained without reduction. Due to its unique two-dimensional structure, good conductivity and large specific surface area, graphene has an important application value in electrochemical detection and electrochemical sensors. The two-dimensional structure of graphene makes graphene a good electrode modification material, which can be used in the preparation of electrochemical sensors and biosensors. Based on ionic liquids (1-butylpyridinium hexafluorophosphate, BPPF6), modified carbon paste electrodes are substrate electrodes. By Using a controlled electrochemical reduction process in the modification of the membrane surface, and using the rest of the electrode surface carboxyl amino-modified probe by an amide linkage fixed on the electrode surface, the preparation of a new type of electrochemical sensor is achieved. Methylene blue is used as the indicator to test the target sequence of the hybridization reaction. The sensor detects the genetic sequence of genetically modified soybean.

2. EXPERIMENTAL

1-Butylpyridinium hexafluorophosphate (BPPF6) was purchased from Alading Co. Ltd. Graphite powder was purchased from Shanghai Colloid Chemical Co., Ltd. Ethyl (3-dimethylaminopropyl) carbodiimine hydrochloride (EDC) and N-hydroxyl imide were purchased from Sigma. Probe ssDNA, target ssDNA, mismatched ssDNA and noncomplementary sequence DNA (ncDNA) were synthesized by Shanghai Sangon Biological Engineering Tech. Co., Ltd. with the following base sequences:

probe ssDNA: 5′-NH_2-CGG TCC TCC GAT CGC CCT TCC-3′,

target ssDNA: 5′-GGA AGG GCG ATC GGA GGA CCG-3′,
one-base mismatched ssDNA: 5′-GGA AGG GCG AAC GGA GGA CCG-3′,
three-base mismatched ssDNA: 5′-GTA AGG GCG AAC GGA GGA CTG-3′, and
ncDNA: 5′-ATC CTT TGC CAT TAC CCG GTA-3′.
The PCR amplification primer sequence of transgenic soybean A2704-12 is written below:
Primer F: 5′-GCA AAA AAG CGG TTA GCT CCT-3′,
Primer R: 5′-ATT CAG GCT GCG CAA CTG TT-3′, and
0.05 M PBS and 0.2 M Tris-HCl buffer were used as the electrolyte.

All electrochemical experiments were performed on a CHI 770E electrochemical workstation (Shanghai CH Instrument, China). A conventional three-electrode system was used with a modified carbon paste electrode as the working electrode, a platinum wire as the auxiliary electrode and a saturated calomel electrode (SCE) as the reference electrode.

Electrodes were produced out by mixing carbon powder with BPPF6. Then, a certain amount of GO solution was dropped on the electrode surface and reduced at -1.5 V in PBS. The prepared electrode was denoted as RGO/CPE.

For fabricating the DNA sensor, RGO/CPE was inserted into 5 mM EDC and 8 mM NHS solution for half an hour. Then, 10 μL of probe ssDNA solution was dropped on the electrode surface and dried naturally. Next, the electrode was washed with 0.5% SDS and water to remove the unconsolidated probe ssDNA. This electrode was denoted as ssDNA/RGO/CPE. Then, 10 μL of target ssDNA was dropped on the above electrode for hybridization and washed with 0.5% SDS and water. This electrode was denoted as dsDNA/RGO/CPE. During sensing, the dsDNA/RGO/CPE was immersed into Tris-HCl solution containing 0.2 mM methylene blue (MB) for scanning.

3. RESULTS AND DISCUSSION

There are many oxygen-containing groups on the surface of GO, such as hydroxyl, carbonyl and carboxyl groups, which have good water solubility but poor conductivity. By controlling the reduction time on the surface of the electrode, it can not only restore part of the conductivity but also retain some oxygen-containing groups on the surface of the electrode [53–57]. Normally, $[Ru(NH_3)_6]^{3+}$, which can bind to phosphodiester groups of DNA molecules through electrostatic adsorption, has been widely used to quantify surface-confined DNA, so we first employed an electrochemical technique to characterize the status of DNA strands on the electrode surface by using $[Ru(NH_3)_6]^{3+}$ as a signaling transducer [58]. In this work, $K_3[Fe(CN)_6]$ is used as a probe for analysis. Figure 1 shows the cyclic voltammetry of the modified electrode in $K_3[Fe(CN)_6]$ solution, which is obtained by the reduction of RGO/CPE at - 1.5 V. It can be seen from the figure that the redox current increases gradually with the reduction time from 0 to 300 s and then remains unchanged. The above result indicates that the oxygen-containing groups on the electrode surface are reduced gradually with the extension of reduction time; thus, the interface conductivity increases gradually. A time of 250 s was selected as the reduction condition, under which enough oxygen-containing groups were ensured to be reduced and restore the good conductivity of graphite.

Figure 2A shows the cyclic voltammograms of differently modified electrodes in a 1 mM $K_3[Fe(CN)_6]$ solution. There is a good redox peak in the CPE curve, and the peak potential difference is 90 mV. On the GO/CPE curve, the current is the smallest because the conductivity of go itself is poor. The electrode surface contains a large number of oxygen-containing groups that make it negatively charged, and the negative redox electrons will also undergo electrostatic repulsion.

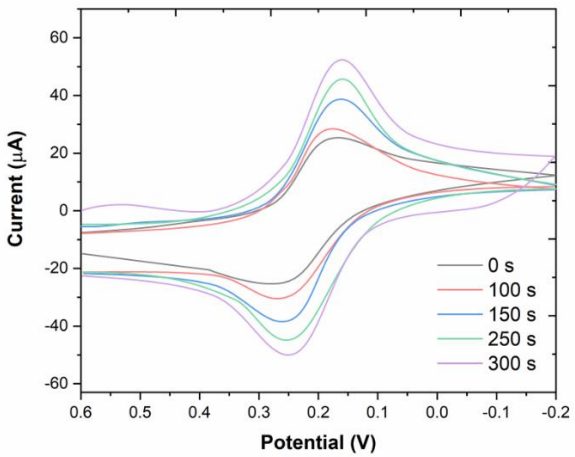

Figure 1. CVs of different reduction time of the RGO/CPE in a 1 mM $K_3[Fe(CN)_6]$ solution at scan rate of 100 mV/s.

However, the peak current on the RGO/CPE curve obviously increases, and the potential difference is 70 mV. This is due to the high conductivity of partially reduced graphite, which greatly increases electron transfer, and the conjugation effect with the aromatic ring of the ionic liquid can make it more stable on the electrode surface [59–64]. When ssDNA is fixed on RGO/CPE, the peak current decreases because of the electrostatic repulsion between the negative ssDNA and the negative redox electron pair.

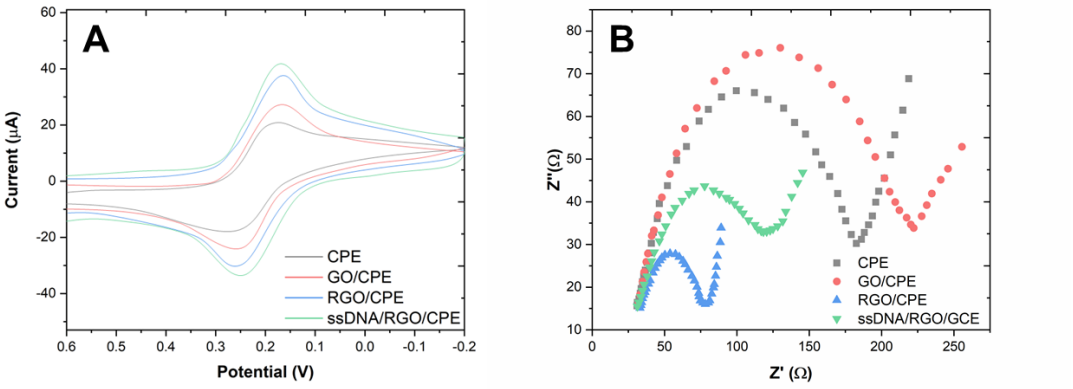

Figure 2. (A) CVs and (B) EIS of different modified electrode in a 1 mM $K_3[Fe(CN)_6]$ solution at scan rate of 100 mV/s. 1: CPE, 2: GO/CPE, 3: RGO/CPE, 4:ssDNA/RGO/CPE.

Electrochemical impedance spectroscopy (EIS) is often used to characterize the surface modification process of electrodes. The semicircle in the high frequency region represents the speed of the redox reaction due to electron transfer on the surface of the electrode, and its size is equal to the value of EIS. Figure 2B shows the electrochemical impedance spectroscopy of differently modified electrodes in 1 mM $K_3[Fe(CN)_6]$ solution. On the CPE curve, the Ret value is 150 Ω. When the weakly conductive GO is modified on the electrode surface, the Ret value increases to 191 Ω. When the GO on the electrode surface is reduced, the Ret value decreases to 51 Ω, indicating that the existence of RGO reduces the interfacial resistance and increases the electron transfer rate of the redox pair on the electrode surface. When the ssDNA probe is fixed on the electrode surface, the Ret value increases to 87 Ω. This is because the phosphate backbone of DNA has a negative charge, which can repel the redox pair with a negative charge and hinder electron transfer on the electrode surface.

In the absence of Hg^{2+}, a rigid duplex pushes the thionine molecule far from β-CD; additionally, the probe can cross through the interspaces within the β-CDs and reach the gold electrode to produce an oxidative current. In the presence of Hg^{2+}, the dsDNA unwinds, and Hg^{2+} combines with T oligonucleotides in A_1 to form a "T–Hg^{2+}–T" construction because the "T–Hg^{2+}–T" conjunction is more stable than the covalent bond between the base pairs in the oligonucleotides [65]. In this work, MB is a kind of phenothiazine dye that is often used as a hybridization indicator in electrochemical DNA sensors. There are three ways to combine MB with DNA. MB can electrostatically adsorb on the phosphate skeleton of DNA, embed in the size groove of the dsDNA double helix structure, or demonstrate an affinity with the base in ssDNA. Because of different DNA sequences and experimental conditions, there are different binding modes between MB and DNA. Figure 3 shows the differential pulse voltammetry of MB on differently modified electrodes. The thiazine group of MB is electrochemical, and the reduction peak appears at - 0.28 V. The reduction peak current of MB on ssDNA/RGO/CPE is larger than that on ssDNA/GO/CPE. At the same time, the current of MB on dsDNA/RGO/CPE is larger than that on dsDNA/GO/CPE, which is due to the good conductivity of RGO. Because the ssDNA probe is located on the electrode surface by covalent bonds, after hybridization, RGO is more easily inserted in the double helix structure with a trench towel size, which makes the signal of MB on the dsDNA-modified electrode larger than that of ssDNA on the modified electrode. The difference in MB current between dsDNA/RGO/CPE and dsDNA/GO/CPE indicates that MB can effectively distinguish single- and double-stranded DNA on the electrode surface.

The selectivity of the sensor was investigated by hybridization of ssDNA/RGO/CPE with different target sequences and recording the reduction current of MB. Figure 4 shows the differential pulse voltammetry of MB at different electrodes. On the ssDNA/RGO/CPE curve, the electrostatic adsorption between MB and ssDNA causes MB to have a small current response. When ssDNA/RGO/CPE is hybridized with non-complementary sequences, the current response of MB increases slightly, which is due to the nonspecific adsorption of ssDNA on the electrode surface. The MB current is 1.4 times that of MB after hybridization with a single base mismatch sequence but less than that of MB after hybridization with a complementary sequence, which indicates that the constructed DNA sensor has good selectivity for different sequences and can distinguish different base mismatch sequences.

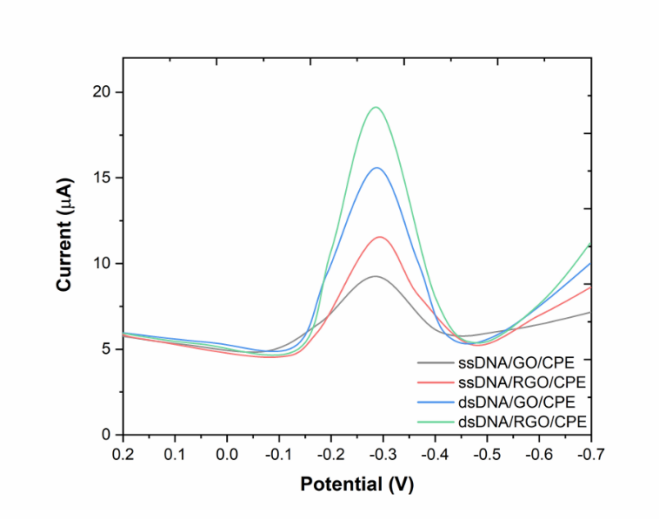

Figure 3. DPVs of (a) ssDNA/GO/CPE, (b) ssDNA/RGO/CPE, (c) dsDNA/GO/CPE and (d) dsDNA/RGO/CPE using MB as the indicator in Tris-HCl buffer solution.

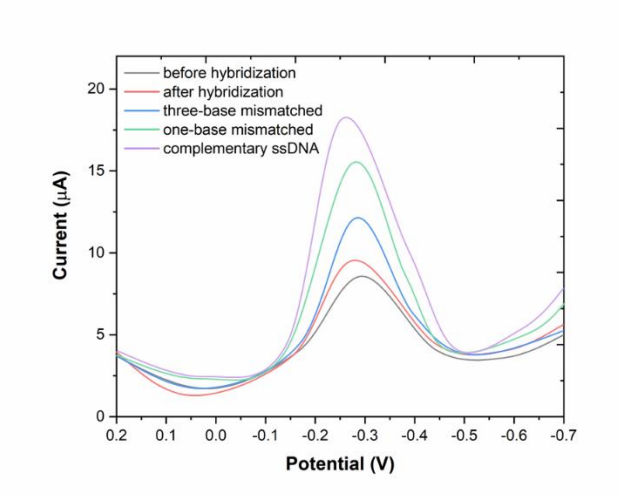

Figure 4. DPVs of MB at ssDNA/RGO/CPE (1) before and after hybridization with (2) noncomplementary sequence, (3) three-base mismatched sequence, (4) one-base mismatched sequence and (5) complementary ssDNA sequence.

The sensitivity of the constructed sensor was studied by investigating the response current of MB after hybridization of ssDNA/RGO/CPE with different concentrations of A2704-12 gene sequences. The results are shown in Figure 5. It can be seen from the figure that the reduction peak current value of MB increases with the increase in the concentration of the target sequence, and there is a good linear relationship between the reduction peak current value and the target sequence concentration in the concentration range of 3 pM-0.5 μM. The detection limit is 1.7 pM, and this result has a higher detection range than those in most methods that have been previously reported (Table 1).

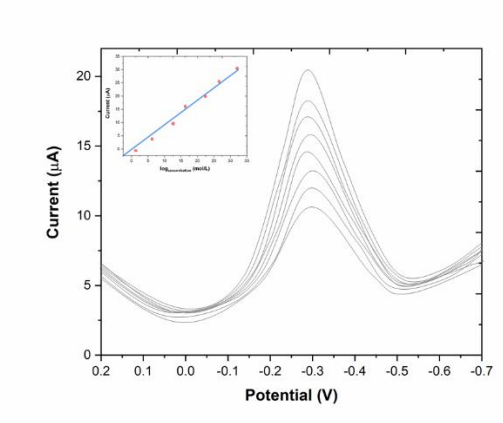

Figure 5. DPVs of MB at ssDNA/RGO/CPE after hybridization with different concentrations of target ssDNA sequence. Inset: plots of Ip versus logarithm of target ssDNA concentration.

Table 1. Comparison of the present method with other reported methods.

Detection methods	Linear range (M)	Detection limit (M)	Reference
Polymerase chain reaction (PCR)	1 to 5000 nM	0.3 nM	[66]
Electrochemical luminescence method (ECL)	5 to 500 fM	1.2 fM	[67]
Recombinase polymerase amplification (RPA)	0.1 pM to 10 nM	1.3 pM	[68]
Fluorescence	10 pM to 10 nM	0.4 pM	[69]
Chronopotentiometry	1 pM to 100 nM	0.45 pM	[70]
ssDNA/RGO/CPE	3 pM-0.5 μM	1.7 pM	This work

The PCR products of the A2704-12 gene sequence are detected by the established method, and the results are shown in Figure 6. After the hybridization of ssDNA/RGO/CPE with the modified A2704-12 gene sequence, the reduction peak current of MB increases significantly compared with that before the hybridization, indicating that the PCR amplification product after denaturation reacted with the electrode containing the same probe sequence, and the dsDNA that formed on the electrode surface combined with more MB molecules. The difference in the MB peak current before and after hybridization indicates that the constructed electrochemical DNA sensor can be used to detect the A2704-12 gene sequence of actual soybean samples.

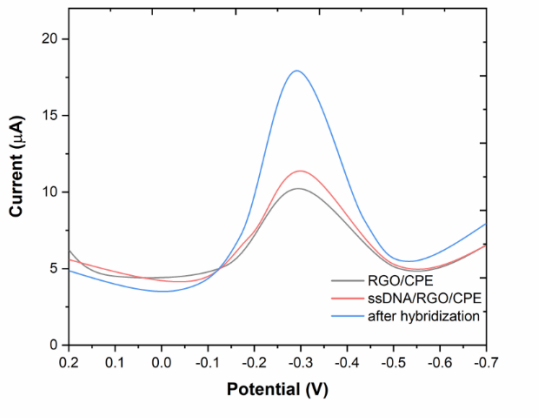

Figure 6. DPVs of MB on (1) RGO/CPE, (2) at ssDNA/RGO/CPE and (3) at ssDNA/RGO/CPE after hybridized with PCR product of A2704-12 gene.

4. CONCLUSION

The surface of a CPE electrode was modified with partially reduced graphite oxide by controlling the electrochemical reduction conditions. Furthermore, DNA electrochemical sensors were prepared by covalently binding an amino-modified probe sequence to the electrode surface. The high conductivity of the RGO on the electrode surface can accelerate electron transfer; thus, the sensitivity of the wall sensor is increased. The proposed DNA sensor has been successfully applied toward the detection of PCR products in transgenic soybean samples.

ACKNOWLEDGEMENT
This work was supported by the Key Natural Science Research Project of Bengbu University: Study of the Key Processing Technology and the Quality Management System Towards the Preparation of soybean Vegetarian Ham (2017ZR03zd).

References

1. N. Hong, L. Cheng, B. Wei, C. Chen, L.L. He, J. Ceng, H.-F. Cui, H. Fan, *Biosens. Bioelectron.*, 91 (2017) 110–114.
2. J. Li, E.-C. Lee, *Sens. Actuators B Chem.*, 239 (2017) 652–659.
3. K. Deng, C. Li, H. Huang, X. Li, *Sens. Actuators B Chem.*, 238 (2017) 1302–1308.
4. S. Wang, F. Yang, D. Jin, Q. Dai, J. Tu, Y. Liu, Y. Ning, G.-J. Zhang, *Anal. Chem.*, 89 (2017) 5349–5356.
5. L. Ribovski, V. Zucolotto, B.C. Janegitz, *Microchem. J.*, 133 (2017) 37–42.
6. H. Teymourian, A. Salimi, S. Khezrian, *Electroanalysis*, 29 (2017) 409–414.
7. Y. Wang, H. Sauriat-Dorizon, H. Korri-Youssoufi, *Sens. Actuators B Chem.*, 251 (2017) 40–48.
8. Y. Ye, J. Gao, H. Zhuang, H. Zheng, H. Sun, Y. Ye, X. Xu, X. Cao, *Microchim. Acta*, 184 (2017) 245–252.
9. M. Cui, Y. Wang, H. Wang, Y. Wu, X. Luo, *Sens. Actuators B Chem.*, 244 (2017) 742–749.
10. A.M. Mohammed, I.J. Ibraheem, A. Obaid, M. Bououdina, *Sens. Bio-Sens. Res.*, 15 (2017) 46–52.

11. Y. Ye, Y. Liu, S. He, X. Xu, X. Cao, Y. Ye, H. Zheng, *Sens. Actuators B Chem.*, 272 (2018) 53–59.
12. Q. Gong, Y. Wang, H. Yang, *Biosens. Bioelectron.*, 89 (2017) 565–569.
13. A. Hájková, J. Barek, V. Vyskočil, *Bioelectrochemistry*, 116 (2017) 1–9.
14. L. Krejcova, L. Richtera, D. Hynek, J. Labuda, V. Adam, *Biosens. Bioelectron.*, 97 (2017) 384–399.
15. H.L.L. Yu, A. Maslova, I. Hsing, *ChemElectroChem*, 4 (2017) 795–805.
16. S. Shahrokhian, R. Salimian, *Sens. Actuators B Chem.*, 266 (2018) 160–169.
17. J. Chen, B. Fu, T. Liu, Z. Yan, K. Li, *Electroanalysis*, 30 (2018) 288–295.
18. V.R.-V. Montiel, R.M. Torrente-Rodríguez, G.G. de Rivera, A.J. Reviejo, C. Cuadrado, R. Linacero, F.J. Gallego, S. Campuzano, J.M. Pingarrón, *Sens. Actuators B Chem.*, 245 (2017) 895–902.
19. A. Purwidyantri, C.-H. Chen, L.-Y. Chen, C.-C. Chen, J.-D. Luo, C.-C. Chiou, Y.-C. Tian, C.-Y. Lin, C.-M. Yang, H.-C. Lai, *J. Electrochem. Soc.*, 164 (2017) B205–B211.
20. Y.-X. Chen, K.-J. Huang, F. Lin, L.-X. Fang, *Talanta*, 175 (2017) 168–176.
21. S.S. Mahshid, F. Ricci, S.O. Kelley, A. Vallée-Bélisle, *ACS Sens.*, 2 (2017) 718–723.
22. R. Hajian, Z. Tayebi, N. Shams, *J. Pharm. Anal.*, 7 (2017) 27–33.
23. N. Gao, F. Gao, S. He, Q. Zhu, J. Huang, H. Tanaka, Q. Wang, *Anal. Chim. Acta*, 951 (2017) 58–67.
24. H.Y. Lau, H. Wu, E.J. Wee, M. Trau, Y. Wang, J.R. Botella, *Sci. Rep.*, 7 (2017) 38896.
25. L. Fu, H. Zhang, Y. Zheng, H. Zhang, Q. Liu, *Rev. Mex. Ing. Quím.*, 19 (2020) 803–812.
26. Y. Xu, Y. Lu, P. Zhang, Y. Wang, Y. Zheng, L. Fu, H. Zhang, C.-T. Lin, A. Yu, *Bioelectrochemistry*, 133 (2020) 107455.
27. L. Fu, A. Wang, H. Zhang, Q. Zhou, F. Chen, W. Su, A. Yu, Z. Ji, Q. Liu, *J. Electroanal. Chem.*, 855 (2019) 113622.
28. L. Fu, A. Wang, K. Xie, J. Zhu, F. Chen, H. Wang, H. Zhang, W. Su, Z. Wang, C. Zhou, S. Ruan, *Sens. Actuators B Chem.*, 304 (2020) 127390.
29. J. Ying, Y. Zheng, H. Zhang, L. Fu, *Rev. Mex. Ing. Quím.*, 19 (2020) 585–592.
30. L. Fu, K. Xie, D. Wu, A. Wang, H. Zhang, Z. Ji, *Mater. Chem. Phys.*, 242 (2020) 122462.
31. L. Fu, K. Xie, A. Wang, F. Lyu, J. Ge, L. Zhang, H. Zhang, W. Su, Y.-L. Hou, C. Zhou, C. Wang, S. Ruan, *Anal. Chim. Acta*, 1081 (2019) 51–58.
32. M. Lutfi Yola, N. Atar, *Curr. Anal. Chem.*, 13 (2017) 13–17.
33. L. Karadurmuz, S. Kurbanoglu, B. Uslu, S. A Ozkan, *Curr. Pharm. Anal.*, 13 (2017) 195–207.
34. S. Jin, Z. Ye, Y. Wang, Y. Ying, *Sci. Rep.*, 7 (2017) 43175.
35. S. Moura-Melo, R. Miranda-Castro, N. de-los-Santos-Álvarez, A. Miranda-Ordieres, J. dos Santos Junior, R. da Silva Fonseca, M. Lobo-Castañón, *Sensors*, 17 (2017) 881.
36. C. He, Y. Tang, S. Wang, J. Liu, Y. Chen, Y. Dong, H. Su, T. Tan, *Anal. Sci.*, 33 (2017) 1155–1160.
37. C.L. Manzanares-Palenzuela, J. Martín-Clemente, M.J. Lobo-Castañón, B. López-Ruiz, *Talanta*, 164 (2017) 261–267.
38. X. Niu, W. Zheng, C. Yin, W. Weng, G. Li, W. Sun, Y. Men, *J. Electroanal. Chem.*, 806 (2017) 116–122.
39. A. Plácido, C. Pereira, A. Guedes, M.F. Barroso, R. Miranda-Castro, N. de-los-Santos-Álvarez, C. Delerue-Matos, *Biosens. Bioelectron.*, 110 (2018) 147–154.
40. B. Martín-Fernández, C.L. Manzanares-Palenzuela, M. Sánchez-Paniagua López, N. de-los-Santos-Álvarez, B. López-Ruiz, *Crit. Rev. Food Sci. Nutr.*, 57 (2017) 2758–2774.
41. S. Jin, Z. Ye, Y. Wang, Y. Ying, *Sci. Rep.*, 7 (2017) 43175.
42. K. Wang, H. Liu, L. Du, X. Ye, *Plant Biotechnol. J.*, 15 (2017) 614–623.
43. R. Banerjee, J. Hasler, R. Meagher, R. Nagoshi, L. Hietala, F. Huang, K. Narva, J.L. Jurat-Fuentes, *Sci. Rep.*, 7 (2017) 10877.

44. L. Fu, Y. Zheng, P. Zhang, H. Zhang, M. Wu, H. Zhang, A. Wang, W. Su, F. Chen, J. Yu, W. Cai, C.-T. Lin, *Bioelectrochemistry*, 129 (2019) 199–205.
45. Y. Zheng, Y. Huang, H. Shi, L. Fu, *Inorg. Nano-Met. Chem.*, 49 (2019) 277–282.
46. L. Fu, M. Wu, Y. Zheng, P. Zhang, C. Ye, H. Zhang, K. Wang, W. Su, F. Chen, J. Yu, A. Yu, W. Cai, C.-T. Lin, *Sens. Actuators B Chem.*, 298 (2019) 126836.
47. F. Meng, Y. Li, Z. Zang, N. Li, R. Ran, Y. Cao, T. Li, Q. Zhou, W. Li, *Pest Manag. Sci.*, 73 (2017) 2447–2455.
48. S.O. Duke, A.M. Rimando, K.N. Reddy, J.V. Cizdziel, N. Bellaloui, D.R. Shaw, M.M. Williams, J.E. Maul, *Pest Manag. Sci.*, 74 (2018) 1166–1173.
49. W. Ning, H. Zhai, J. Yu, S. Liang, X. Yang, X. Xing, J. Huo, T. Pang, Y. Yang, X. Bai, *Mol. Breed.*, 37 (2017) 19.
50. R. Fuganti-Pagliarini, L.C. Ferreira, F.A. Rodrigues, H.B. Molinari, S.R. Marin, M.D. Molinari, J. Marcolino-Gomes, L.M. Mertz-Henning, J.R. Farias, M.C. de Oliveira, *Front. Plant Sci.*, 8 (2017) 448.
51. Y. Yang, Y. Zhou, Y. Chi, B. Fan, Z. Chen, *Sci. Rep.*, 7 (2017) 17804.
52. Q. Du, X. Yang, J. Zhang, X. Zhong, K.S. Kim, J. Yang, G. Xing, X. Li, Z. Jiang, Q. Li, *Transgenic Res.*, 27 (2018) 277–288.
53. R. Shi, J. Liang, Z. Zhao, A. Liu, Y. Tian, *Talanta*, 169 (2017) 37–43.
54. Y. Zhu, D. Pan, X. Hu, H. Han, M. Lin, C. Wang, *Sens. Actuators B Chem.*, 243 (2017) 1–7.
55. H. Bagheri, A. Hajian, M. Rezaei, A. Shirzadmehr, *J. Hazard. Mater.*, 324 (2017) 762–772.
56. J. Wang, B. Yang, J. Zhong, B. Yan, K. Zhang, C. Zhai, Y. Shiraishi, Y. Du, P. Yang, *J. Colloid Interface Sci.*, 497 (2017) 172–180.
57. Y. Liang, L. Yu, R. Yang, X. Li, L. Qu, J. Li, *Sens. Actuators B Chem.*, 240 (2017) 1330–1335.
58. J. Zhao, M. Xin, Y. Cao, Y. Yin, Y. Shu, W. Ma, *Anal. Chim. Acta*, 860 (2015) 23–28.
59. Y.V.M. Reddy, S. Bathinapatla, T. Łuczak, M. Osińska, H. Maseed, P. Ragavendra, L.S. Sarma, V. Srikanth, G. Madhavi, *New J. Chem.*, 42 (2018) 3137–3146.
60. A. Benvidi, M.T. Nafar, S. Jahanbani, M.D. Tezerjani, M. Rezaeinasab, S. Dalirnasab, *Mater. Sci. Eng. C*, 75 (2017) 1435–1447.
61. H. Wang, S. Zhang, S. Li, J. Qu, *Talanta*, 178 (2018) 188–194.
62. M. Baccarin, F.A. Santos, F.C. Vicentini, V. Zucolotto, B.C. Janegitz, O. Fatibello-Filho, *J. Electroanal. Chem.*, 799 (2017) 436–443.
63. N. Akkarachanchainon, P. Rattanawaleedirojn, O. Chailapakul, N. Rodthongkum, *Talanta*, 165 (2017) 692–701.
64. D. Wang, F. Xu, J. Hu, M. Lin, *Mater. Sci. Eng. C*, 71 (2017) 1086–1089.
65. J. Li, M. Sun, X. Wei, L. Zhang, Y. Zhang, *Biosens. Bioelectron.*, 74 (2015) 423–426.
66. T.S. Bronder, M.P. Jessing, A. Poghossian, M. Keusgen, M.J. Schöning, *Anal. Chem.*, 90 (2018) 7747–7753.
67. Y. Wang, D. Shan, G. Wu, H. Wang, F. Ru, X. Zhang, L. Li, Y. Qian, X. Lu, *Biosens. Bioelectron.*, 106 (2018) 64–70.
68. *Biosens. Bioelectron.*, 54 (n.d.) 674–678.
69. S. Takalkar, K. Baryeh, G. Liu, *Biosens. Bioelectron.*, 98 (2017) 147–154.
70. D. Chen, M. Zhang, M. Ma, H. Hai, J. Li, Y. Shan, *Anal. Chim. Acta*, 1078 (2019) 24–31.